Journal of Power Sources 480 (2020) 228867

Contents lists available at ScienceDirect

Journal of Power Sources

journal homepage: www.elsevier.com/locate/jpowsour

Perspective

Device modeling and performance optimization of thermoelectric generators under isothermal and isoflux heat source condition

Mani Ranjan, Tanmoy Maiti *

Plasmonics and Perovskites Laboratory, Department of Materials Science and Engineering, Indian Institute of Technology, Kanpur, UP, 208016, India

HIGHLIGHTS

- Numerical model of TEG provides insight into the contribution of energy losses.
- Finite element modeling for TEG under isothermal and constant heat source condition.
- Effect of varying leg geometry and energy losses on performance of 196 legged TEG.
- Optimized controlling parameters of TEG using Taguchi and ANOVA methods.

GRAPHICAL ABSTRACT

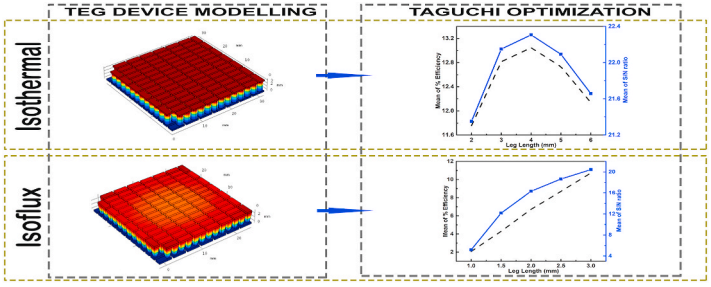

ARTICLE INFO

Keywords:
Thermoelectric generator
Isoflux
Isothermal
Taguchi
ANOVA

ABSTRACT

Thermoelectric generator (TEG) is considered as promising way of clean energy generation by recycling waste heat, but its poor performance due to several kinds of energy losses impedes wide scale commercialization. Since, most of the waste heat sources have constant heat flux (isoflux) conditions it is necessary to evaluate the performance of TEG under such conditions. Here, various kinds of parasitic heat losses such as conduction, and radiation along with energy losses through contacts are numerically simulated in order to predict the performance of TEG for both isothermal and isoflux heat source conditions. Further, optimizations of controlling parameters of TEG such as leg geometry, leg length, cross sectional area, and external load resistance are done to maximize the efficiency and power output of TEG. To overcome the cumbersome optimization process by experimental trials, Taguchi and ANOVA methods are employed to optimize all the device parameters for both types of operating conditions i.e. isothermal and isoflux. Under optimized conditions, maximum power of ~48 W (an increase of 52%) is predicted under isothermal condition for cylindrical legged TEG and 10.6 W (an increase of 100%) is obtained under constant heat flux of 63 kW/m^2 for pyramid legged TEG.

1. Introduction

Currently majority of our energy demands are fulfilled through burning fossil fuels causing enhanced carbon emission leading to increase in greenhouse gases and climate change [1]. On the other hand, a significant amount of energy consumed by us is wasted as heat. Some of the examples of waste heat includes, automotive exhaust, radiating furnace walls, hot combustion gases discharged to atmosphere, heated water released to environment, heated products exiting industrial processes etc. Recently, Firth et al. [2] have estimated that more than 50% of global energy consumption may end up as waste heat in 2030. There

* Corresponding author.
E-mail address: tmaiti@iitk.ac.in (T. Maiti).

https://doi.org/10.1016/j.jpowsour.2020.228867
Received 25 May 2020; Received in revised form 13 August 2020; Accepted 28 August 2020
Available online 7 September 2020

Nomenclature

TE	Thermoelectric
TEG	Thermoelectric Generator
FEM	Finite Element Method
EMF	Electromotive Force
ZT	Dimensionless Figure of Merit
S	Seebeck Coefficient
P	Peltier Coefficient
μ	Thomson Coefficient
σ	Electrical Conductivity
ρ	Electrical Resistivity
k	Thermal Conductivity
T	Temperature
T_h	Hot End Temperature
T_c	Cold End Temperature
η	TEG Efficiency
η_c	Carnot's Efficiency
η_{max}	Thermoelectric Maximum efficiency
ZT_{eng}	Engineering Dimensionless Figure of Merit
$\widehat{\alpha}$	Dimensionless Intensity Factor of Thomson Effect
P_{out}	Electrical Power Output
Q_{in}	Heat flowing into the TEG
q_c	Conductive Heat Flux
q	Total Heat Flux
q_{gen}	Heat flux Generated
q_{rad}	Heat flux lost due to radiation
J	Electric Current Flux
∇T	Temperature Gradient
∇V	Potential Gradient
d	Density
C_p	Heat Capacity
ρ_{sc}	Space Charge Density
G	Incoming Radiative Heat Flux (or Irradiation)
G_m	Mutual Irradiation
F_{amb}	View Factor
ε	Emissivity
σ_{SB}	Stefan-Boltzmann Constant
ρ_C	Thermal Contact Resistance
ρ_S	Electrical Contact Resistance
S/N	Signal to Noise Ratio
R	Total no. of Repetitions
CI	Confidence Interval
OA	Orthogonal Array

is a huge potential for utilizing these waste heat via thermoelectric generators (TEGs), which can convert directly heat into electricity without having any moving parts or chemical discharge. TEGs comprising of n-type and p-type thermoelectric legs sandwiched under insulating ceramic substrates have been fabricated and studied in the past [3–5]. The performance of any thermoelectric (TE) material is defined by its figure of merit (ZT) which is given by $ZT = \frac{S^2\sigma}{k}T$, where T is temperature, S is Seebeck coefficient, σ is electrical conductivity and k is thermal conductivity of the material. The maximum efficiency of any thermal device is defined by Carnot efficiency, $\eta_c = \frac{T_h - T_c}{T_h}$, where T_h and T_c are the temperatures of hot and cold end, respectively. But in case of TE materials, maximum efficiency is constrained by interdependent properties of material. The maximum efficiency of a thermoelectric material is calculated [6] as

$$\eta_{\max} = \eta_c \frac{\sqrt{1 + ZT_{eng}\left(\frac{\widehat{\alpha}}{\eta_c} - \frac{1}{2}\right)} - 1}{\left(\sqrt{1 + ZT_{eng}\left(\frac{\widehat{\alpha}}{\eta_c} - \frac{1}{2}\right)} + 1\right) - \eta_c} \quad (1)$$

where, ZT_{eng} is the engineering dimensionless figure of merit defined as $(ZT)_{eng} = \frac{\left(\int_{T_c}^{T_h} S(T)dT\right)^2}{\int_{T_c}^{T_h}\rho(T)dT \int_{T_c}^{T_h} k(T)dT}\Delta T$ and, $\widehat{\alpha}$ is a dimensionless intensity factor of the Thomson effect defined as $\widehat{\alpha} = \frac{S(T_h)\ \Delta T}{\int_{T_c}^{T_h} S(T)dT}$, where $S(T_h)$ denotes the value of Seebeck coefficient at hot temperature. Even though good ZT materials are available, high power output and high conversion efficiencies from TEG have not been achieved experimentally as expected. Several computational and theoretical models have been proposed [7–16] to analyze the reasons behind low efficiency obtained in TEG. Models developed for performance evaluation (efficiency and power output) [7,16] have shown that the deviation from experimental results causes due to several effects of heat losses and contact losses. Independent researchers have attributed the primary reason behind poor performance of TEG to various energy losses such as radiative and conductive heat transfers [8], high contact resistance [9] and convective heat losses [10]. However, very few reports are found in literature [17, 18], where combination of all these energy losses have been studied. Furthermore, it has been reported [11,12] that performance of TEG depends on leg geometries such as cylindrical, rectangular, trapezoidal, octahedral etc. Although, these reports have considered the leg geometry variation only for few leg TE module. The effects of the leg geometry in a multilegged TEG environment in combination with various heat loss effects are hardly found in literature. Moreover, all the previous works reported in the literature have been carried out considering an isothermal heat source condition where the hot side is kept at constant temperature. But in practical applications, the waste heat can be constant heat source (isoflux) condition e.g. radiating furnace walls, convective exhaust gas etc. As suggested by Thacher [19], in general the actual operating conditions for a TEG falls between the isothermal and isoflux heat source conditions.

In the present work, using finite element modeling we have demonstrated the enhancement of power output and efficiency of a TEG consisting of 98 pairs (196 legs) of p-n type TE legs by optimizing the leg geometry taking into consideration with different kinds of energy losses under both isothermal and isoflux heat source condition. To the best of our knowledge, this is the first report on the effect of various leg geometries coupled with various energy losses on the performance of a TEG under isoflux condition.

Furthermore, it is apparent from the recent reports [20,21] that many other parameters such as leg dimensions, leg spacing, external load resistance, ambient temperature etc. control the performance of TEG. It remains a challenge to optimize all these factors experimentally for maximizing the performance of TEG since the number of experimental trials necessary for optimization of all the controlling parameters is quite exhaustive. Taguchi method has been widely used to optimize operational variables because of its unique discipline that requires a very minimum number of experiments. Taguchi method has been used at many instances for the optimization of process parameters such as for improving the surface roughness of lathe facing operation [22], diesel-engine system design [23], removal of copper and nickel by growing *Aspergillus* [24] etc. In the field of TEG, Chen et al. [13] have used Taguchi method to optimize the dimensions of heat sink while Kishore et al. [14,15] have used Taguchi and ANOVA methods for TE device optimization. However, all these works on TEG device optimization have been carried out considering an isothermal heat source

condition where the hot side is kept at constant temperature, typically less than 500 K. No such report has been found in the literature on TEG performance optimization under isoflux heat source condition.

In the present investigation, we have optimized the configuration of TEG under both isothermal (800 K) and isoflux heat source conditions (63 kW/m^2) using Taguchi and ANOVA methods by controlling various parameters such as leg length, cross sectional area, and load resistance under consideration of various energy losses. Finite element model of TEG has been developed in COMSOL Multiphysics, using p-type $Pb_{0.98}Na_{0.02}Te$-8%SrTe (ZT of 2.3 at 800 K) [25] and n-type material $AgPb_{18}SbTe_{20}$ (ZT of 2.2 at 800 K) [26].

2. TEG model and numerical formulations

2.1. Thermoelectric generator

A thermoelectric generator (TEG) is an assembly of several thermoelectric modules (TEM), having n- and p-type thermoelectric legs, in which the legs are electrically connected in series and thermally in parallel. As the material is subjected to temperature gradient, charge carriers i.e. electrons in n-type materials and holes in p-type materials, diffuses from hot end to cold end until an equilibrium is reached between the diffusion potential and the electrostatic repulsion potential, resulting a built-in voltage known as Seebeck effect [27]. The top and bottom sides of the module are often covered with substrates, which have high thermal conductance and electrical resistivity such as Aluminium Oxide (Al_2O_3) or Aluminium Nitride (AlN). The substrate not only ensures a good thermal contact but also supports the mechanical integrity of the system. The efficiency of the TEG is calculated as,

$$\eta = \frac{P_{out}}{Q_{in}} \tag{2}$$

where, P_{out} is the electric power output and Q_{in} is the heat flowing into the TEG.

A 4 cm × 4 cm model of a thermoelectric generator consisting of 98 pairs (196 legs) of p-n square based legs has been initially created in COMSOL Multiphysics. The heat transfer equations, electric current and thermoelectric equations are implemented in order to calculate the TEG power output and energy conversion efficiency. The model assumes p- and n-type legs connected electrically in series and thermally in parallel. In the present work we chose $Pb_{0.98}Na_{0.02}Te$-8%SrTe (ZT of 2.3 at 800 K) [25] and $AgPb_{18}SbTe_{20}$ (ZT of 2.2 at 800 K) [26] as p- and n-type materials respectively, since their *ZT* values are comparable and these are very high *ZT* values reported in literature. TE legs are connected electrically with Cu electrodes of thickness 0.5 mm.

First, a square based leg of size 1.4 mm × 1.4 mm x 2 mm has been created and simulated for the following cases: no heat loss condition, radiation heat loss condition, conduction heat loss condition, contact loss condition and combined energy loss condition. TEG model is then optimized for various leg geometries such as square based, cylindrical leg, conical frustum, and pyramid frustum. The leg spacing and substrate has been kept fixed at 5 mm and 4 cm × 4 cm respectively. For the top hot end, two types of heat sources namely isothermal (constant temperature of 800 K) and isoflux (constant heat flux of 63 kW/m^2) heat sources have been assumed while the bottom end is fixed at 293 K. Thermoelectric effect is mainly comprised of the Seebeck effect (EMF generation in presence of temperature gradient), Peltier effect (cooling effect in presence of an EMF) and Thomson effect (heating or cooling effect in a temperature gradient). The three effects i.e. Seebeck (*S*), Thomson (μ) and Peltier (P) coefficients are related as

$$P = ST \tag{3}$$

$$\mu = T\frac{dS}{dT} \tag{4}$$

In the model, the conduction heat transfer can be assumed to be equivalent to heat transfer in solids as described by Fourier's law given by

$$q_c = -k\nabla T \tag{5}$$

where, q_c is the conductive heat flux, k is the thermal conductivity and ∇T is the temperature gradient.

The total heat flux (q) and electric current flux (J) can be denoted as

$$q = -k\nabla T + PJ \tag{6}$$

$$J = -\sigma\nabla V - \sigma S\nabla T \tag{7}$$

where, σ is the electrical conductivity and ∇V is the potential gradient. The first term in Eq. (6) denotes the Fourier heat transfer and the second term describes the Peltier effect. On the other hand, the first term in Eq. (7) describes the Ohm's law and the later defines the Seebeck effect [28].

Also, conservation of heat energy and current gives

$$dC_p\frac{\partial T}{\partial t} + \nabla\cdot q = q_{gen} \tag{8}$$

$$\nabla\cdot J = -\frac{\partial \rho_{sc}}{\partial t} \tag{9}$$

where, d is the density, C_p is the heat capacity at constant pressure and ρ_{sc} is the space charge density. At steady state, above equations reduce to

$$\nabla\cdot q = q_{gen} \tag{10}$$

$$\nabla\cdot J = 0 \tag{11}$$

More explicitly, the thermoelectric equation becomes [29].

$$\nabla.(-k\nabla T + P(-\sigma\nabla V - \sigma S\nabla T)) = (-\sigma\nabla V - \sigma S\nabla T)\cdot(-\nabla V) \tag{12}$$

$$\nabla\cdot(-\sigma\nabla V - \sigma S\nabla T) = 0 \tag{13}$$

These equations have been solved on a finite element mesh for T and V and finally obtain the temperature and potential distribution.

In this model, we have introduced various parasitic losses such as conduction heat loss, radiation heat loss from TE legs. We have also considered thermal contact resistance between the leg and Cu electrode and between Cu electrode and Alumina substrate, while electrical contact resistance has been considered between leg and Cu electrode only. The effects of these losses are studied separately and combined together to make the results more realistic. The heat loss through convection has not been considered here as the air flow within such low spaces between the legs can be neglected.

2.2. Conduction heat loss

For considering heat loss through air, a block of size 4 cm × 4 cm x 2 mm has been created exactly such that it just encloses the whole TEG covering the space between the legs and between the ceramic substrates similar to that reported in previous works [8]. The Fourier heat transfer equation as defined by Eq. (5) under steady state conditions are implied to the assumed air block and no heat loss has been considered outside this block.

2.3. Radiation heat loss

The radiation heat loss is also assumed to be constrained within the block i.e. the air volume. The radiation losses from legs and from substrate is assumed to be difference of incoming radiation and the one leaving theses surfaces in the positive outward direction.

$$q_{rad} = \varepsilon\left(G - \sigma_{SB}T^4\right) \tag{14}$$

where, G is the incoming radiative heat flux or irradiation and is defined as

$$G = G_m + F_{amb}\sigma_{SB}T_{amb}^4 \tag{15}$$

where, G_m is mutual irradiation from other surfaces, and F_{amb} is the view factor. ε is the emissivity and is allotted a value of 0.8 [30]. The air block walls have been assumed adiabatic and thus given the properties of diffuse mirrors as per advised by Bjork [8], where $q_{rad} = 0$ and so $G = \sigma_{SB}T^4$.

2.4. Contact losses

The legs are usually connected to the metallic electrodes via welding, brazing or soldering. However many times, contacts have certain asperities or roughness which in turn affects their thermal and electrical conductivity. The heat flux due to the constriction of thermal contact resistance is given by $\dot{q} = \frac{\Delta T}{\rho_C}$ where ρ_C is the thermal contact resistance. The electrical current flux is given by $\dot{J} = \frac{\Delta V}{\rho_S}$, where ρ_S is electrical contact resistance. In this work electric contact loss has been considered only between the leg and electrode contacts, while thermal contact loss has been considered between the legs and the electrodes as well as the loss between the electrodes and ceramic substrates. The available electrical contact resistance and thermal contact resistances in literature [15,18] are in the ranges of $10^{-9} - 10^{-7}$ Ω -m^2 and $10^{-6} - 10^{-4}$ m^{2}K/W respectively. Assuming that one gets very good contacts, in this model we have considered the values of electrical contact resistance and thermal contact resistances to be 10^{-9} Ω -m^2 and 10^{-6} m^{2}K/W respectively.

2.5. Taguchi method

Taguchi method uses a set of predefined orthogonal arrays for design of experiments or process optimization [31]. The choice of orthogonal arrays depends upon the number of factors to study and depth of information to study i.e. number of levels for each control factor. This allows us to reduce the total number of experimental runs. Taguchi has introduced the concept of signal to noise ratio (S/N), where the desirable output is considered as signal and the undesirable output is termed as noise which is also a measure of variability in the process. The S/N ratio indicates the response variation with respect to the target value under different noise conditions. He defined different signal to noise ratios depending on different situations namely larger the better, smaller the better, and on target (minimum variation). In our study the situation is to maximize efficiency and power output so the concept of larger the better situation is used. It is calculated using

$$\text{Larger the better (S/N)ratio} = -10\log\left[\frac{1}{R}\sum_{i=1}^{R}\frac{1}{y_i^2}\right] \tag{16}$$

where R is total number of repetitions in experiment and y_i is the output for i th trial. Here the factor level having highest S/N ratio gives the optimal level of the control factors [32].

The optimized output can then be calculated using

$$Y_{optimal} = \overline{X} + \sum_{i=1}^{m}\left(\overline{X}_i - \overline{X}\right) \tag{17}$$

where $\overline{X}_i$ is mean of output at optimal level and $\overline{X}$ is the total mean of all the outputs [33]. The confidence interval (CI) can be calculated as [34].

$$CI = \left(F_\alpha(1, DF_e)V_e\left[\frac{1}{n_{eff}} + \frac{1}{R}\right]\right)^{1/2} \tag{18}$$

where $F_\alpha(1, DF_e)$ is the F ratio for degree of freedom 1 and error degree of freedom (DF_e), for a CI of $(1-\alpha)$, V_e is the variance in error, and n_{eff} is defined as $n_{eff} = \frac{n}{1+(DF)_T}$, where $(DF)_T$ is the total degrees of freedom in estimation of mean and n is the total number of experiments.

2.6. ANOVA

In the present work we have also used analysis of variance (ANOVA) to analyze the process parameters that affects the performance of the experiment. The total variability of S/N ratios given by sum of squared deviations (SS_T) from mean value is calculated by $SS_T = \sum_{i=1}^{n}(y_i - y_m)^2$ where n is number of experimental runs and y_m is the mean value. F test named after Fisher [35] signifies the effect of control factors on the output of experiment. F value is given by the ratio of the mean of squared deviations to the mean of squared error. A typical ANOVA table comprises of the following terms: degrees of freedom, sum of squares, variance, F-values and percentage contribution of each of the control factors.

3. Results and discussion

The schematics of the TEG created in COMSOL Multiphysics is shown in Fig. 1a. One end of the electrode leg is allotted ground voltage (V = 0), while the other end shows the output voltage (V_{out}). The two ends are assumed to be connected to a certain load resistance during simulation. Tetrahedral meshing is done as shown in Fig. 1b and predefined normal mesh element size is chosen as per Table 1. Temperature and potential distribution within the TEG are shown in Fig. 1d and e respectively. Since the legs are connected thermally in parallel, the temperature distribution across the leg length remains same for legs of the same type. However, the temperature variations in the p- and n-legs are different due to difference in their thermal conductivities as shown in Fig. 1c. The maximum and minimum temperatures are shown as 795 K and 295 K respectively. The potential distribution within the legs is also shown in Fig. 1e and the decrease in potential is clearly evident along the series connection of the legs. The total potential drop between the two ends has been calculated to be approximately 12.5 V.

The performance of the TEG has been evaluated under various energy loss conditions such as conduction, radiation, contact resistance, combination of conduction and radiation and finally under combination of all energy losses. The calculated efficiency and power output as a function of varying load resistances are shown in Fig. 2. The peak in efficiency is obtained at 6 Ω while peak in power output is obtained at 5 Ω. The results clearly show that maximum efficiency is obtained when there are no heat losses. However, efficiency decreases gradually when we consider radiation, contact, conduction, conduction + radiation and combined all energy loss. This order of decrease in efficiency is in sync with what has been reported by Bjork et al. [8].

However, the variation in maximum power output due to various energy loss mechanisms has not been found to follow the same trend what has been obtained for efficiency. Indeed, heat losses do not affect much the power output of TEG as shown in Fig. 2b. However, the power output is reduced significantly due to contact loss. Introduction of electrical and thermal resistance in the interfaces of TE legs and electrodes cause the change in the temperature distribution profile of the TE Legs resulting the decrease in power output when we consider contact loss. It is to be noted that in our simulations lowest reported contact resistance values were considered. However, in practice, the reduction in power output due to the contact loss is expected to be higher than what has been reported here especially since, the contact resistance of actual device can be raised by several factors affecting the quality of the interface such as defects, roughness, strain and composition of the interface. Moreover, radiation heat loss has been found to cause slight increase in power output of TEG. The output power reduced by 4.9% under contact loss, while reduction under combined energy loss

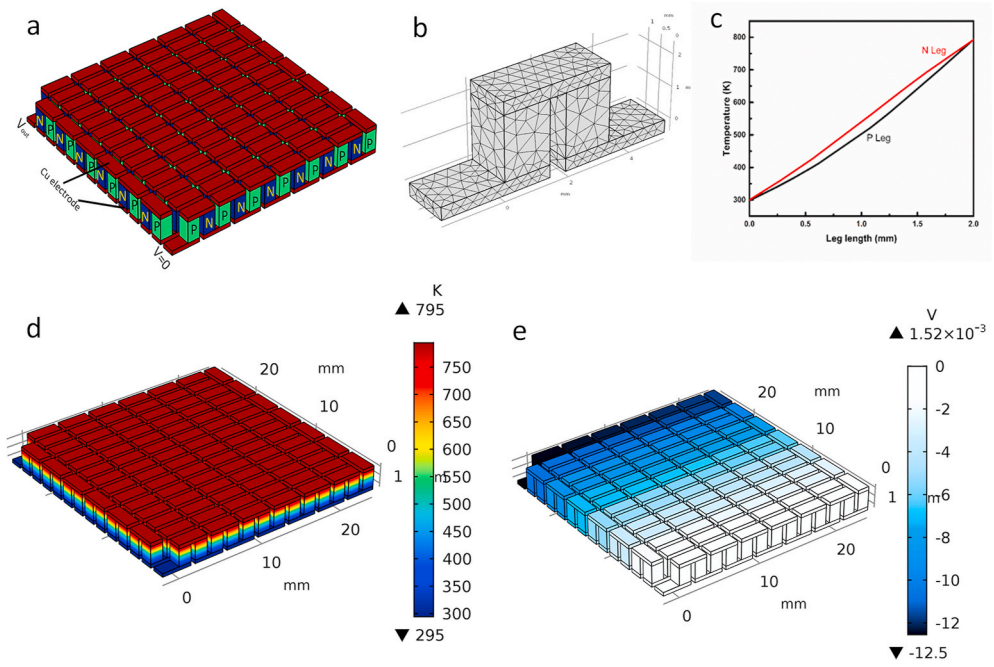

Fig. 1. (a) Schematics of the modelled TEG (Ceramic substrates are removed for better view) where top side is the hot end (800 K) and bottom is the cold end (293 K); (b) Tetrahedral meshing done with normal mesh element size shown for one of the pairs of TE legs; (c) Temperature distribution along 2 mm leg from bottom cold end to top hot end; (d) Temperature variation within the TEG; (e) Potential distribution within the TEG.

Table 1
Mesh Independency test for different leg geometries showing error variation.

	Square base	Cylindrical	Cone up	Cone down	Pyramid up	Pyramid down
Mesh element size	Normal	Fine	Normal	Normal	Coarse	Coarse
% Error	0.024%	0.078%	0.05%	0.053%	0.07%	0.056%

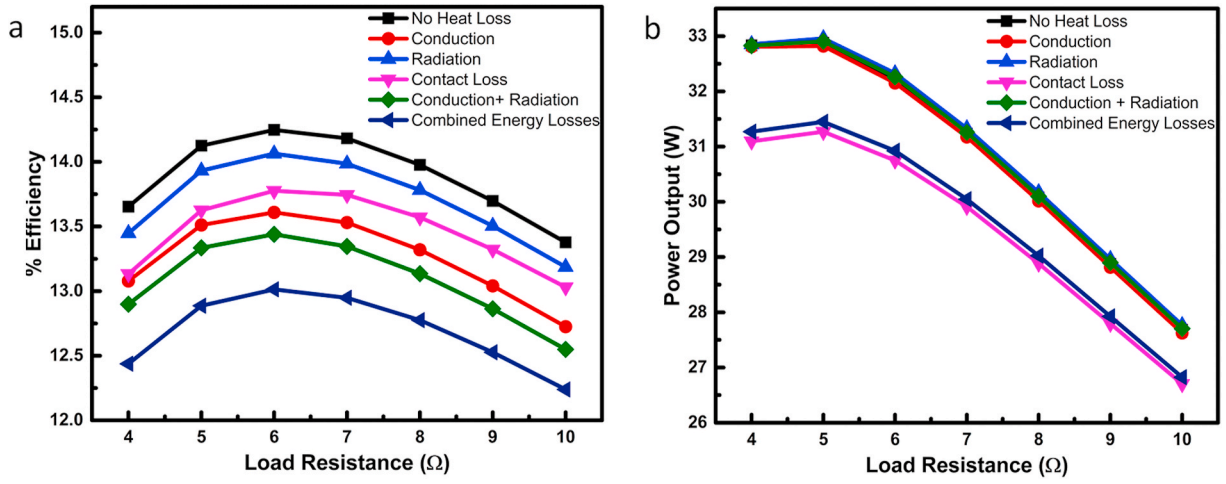

Fig. 2. Modelled TE generator performance considering various heat losses (a) % efficiency variation with load resistance; (b) Power output variation with load resistance.

condition has been found to be only 4.35% at load resistance of 5 Ω. As a result, better power output has been obtained when we consider combined energy losses compared to that obtained for contact losses. The higher value of power output in case of radiation than no heat loss condition can be explained as incoming irradiation from the neighboring TE legs contributing to the net heat flux, thus enhancing energy conversion. In the present investigation we have considered combination of conduction, radiation and contact energy losses for further study, assuming surface emissivity having a constant value of 0.8 and electrical contact resistance and thermal contact resistances to be 10^{-9} Ω -m^2 and 10^{-6} m^2K/W respectively. The effect of leg spacing on the performance has also been studied and the results are shown in Fig. S1 in Supporting Information. The efficiency decreases while, power output increased with increasing leg spacing. The efficiency decreased due to an increase in radiation with increasing leg spacing whereas the total energy conversion increased resulting in greater power output [17].

3.1. Model validation

To further validate our model under energy loss considerations, we have simulated a 142 legged model consisting of $Bi_2Te_{2.7}Se_{0.3}$ and $Zn_xBi_{0.46}Sb_{1.54}Te_{3+x}$ at x = 0.015 as n- and p-type materials respectively, whose experimental results can be found in Ref. [16]. The efficiency and power output obtained in simulation are higher than the experimental results when no heat loss condition is considered. Upon considering various energy losses simulation results have been found to be close to the experimental data as shown in Fig. S2 in Supporting Information. Possible explanations for such discrepancies can be error in experimental results, unavailability of exact emissivity and contact resistivity values and convection effects of heat loss that has not been considered in this model.

3.2. Performance optimization under isothermal heat source condition

3.2.1. Leg geometry optimization

Tetrahedral mesh elements chosen for the simulation have been checked for the effect of mesh sizes on the result. COMSOL Multiphysics offers a list of mesh element size namely fine, normal, coarse, coarser etc. The error obtained for different TE leg geometries under considered mesh element sizes is shown in Table 1.

Different leg geometries have been chosen such as square base, cylindrical, cone-up (larger cross sectional area to the hot end side), cone-down (larger cross sectional area to the cold end side), pyramid-up (larger cross sectional area to the hot end side) and pyramid-down (larger cross sectional area to the cold end side), with bottom to top end area ratio of 2 or ½ for asymmetrical geometries. It is to be noted that the leg geometry of p- and n-type legs ($Pb_{0.98}Na_{0.02}Te$-8%SrTe and $AgPb_{18}SbTe_{20}$ respectively) always remains same in our investigation. Also leg length and leg volume have been kept constant when different thermoelectric leg geometries have been considered. The performance of TEG under isothermal heat condition for different leg geometries upon considering combined energy loss is shown in Fig. 3. The maximum power output ~31.5 W is obtained for cylindrical legs. The difference in the results for square base and cylindrical legs is 0.3%. The results have been checked for different mesh sizes and the conclusion remains the same. However, the efficiency value has been found to be maximum for pyramid-up shaped leg geometry followed by cylindrical, square-base, pyramid-down, cone-up and cone-down. Even though, pyramid-up leg shows maximum efficiency, cylindrical leg has been chosen as optimized leg geometry because of its higher power output. A detailed study done by comparing the results in no heat loss and radiation heat loss condition presented in Table S1 reveals that radiation is the main cause for increased efficiency obtained in the pyramid legs. However, a lot of other factors such as ambient temperature, leg length, load resistance, etc. also affects the performance of the TEG and thus needs to be optimized. Taguchi and ANOVA methods have been chosen for further optimization of these parameters.

3.2.2. Optimization of TEG parameters using Taguchi and ANOVA analysis

The first step in Taguchi optimization involves the identification of control factors and assignment of different control levels. After a lot of literature survey and brain storming, three important control factors have been chosen in the present work such as leg length, leg cross sectional area and load resistance. Five levels of optimization for each parameter have been carried out. The range of these parameters based on initial simulation result trends are taken as 2–4 mm^2 for leg area, 2–6 mm for leg length and 6–10 Ω for load resistance as presented in Table 2.

The next step involves the choice of orthogonal arrays (OAs) as defined by Taguchi, which are selected based on total number of factors and level of each factor. Taguchi's OA based experimental design matrix is denoted as L_N (b^K), where N is number of runs, b is the number of levels in each factor and K is the number of factors. Following the standard orthogonal arrays in Taguchi method [31], in the current work L_{25} array type has been chosen as there are 5 levels in all the three factors considered, which enables us to use only 25 trials to predict the optimal combination rather than $5^3 = 125$ trials. The efficiency and power output obtained for the 25 trials along with their signal to noise (S/N) ratio for 'Larger the Better' condition as per Eq. (16) are shown in Table 3. The mean of the responses for efficiency and power and mean response of their S/N ratios are shown in Table S2 in Supporting Information.

The means of data at all levels of different control factors are plotted in Fig. 4. The highest value of S/N ratio denotes the optimal level in each of these graphs. Thus, one can easily figure out the combinations of $A_2B_3C_2$ (leg area: 2.5 mm^2, leg length: 4 mm and load resistance: 7 Ω) and $A_5B_1C_1$ (leg area: 4 mm^2, leg length: 2 mm and load resistance: 6 Ω) as the optimum conditions for maximum efficiency and power output,

Table 2
Control factors and their levels chosen for optimization.

Control Factors		Units	Level 1	Level 2	Level 3	Level 4	Level 5
A	Leg cross sectional area	mm^2	2	2.5	3	3.5	4
B	Leg length	mm	2	3	4	5	6
C	Load resistance	Ω	6	7	8	9	10

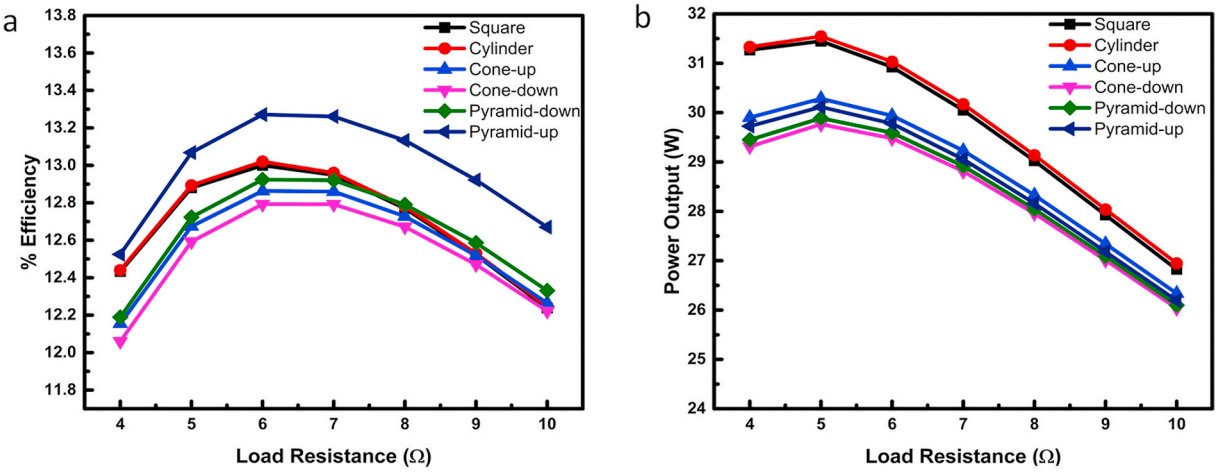

Fig. 3. Geometrical optimization for varying leg geometries under the condition of isothermal heat input (a) Efficiency variation with load resistance; (b) Power output variation with load resistance.

Table 3
Different levels of control factors arranged as per L_{25} orthogonal array. The results (efficiency and power output) of the simulation as per the array is shown along with their S/N ratio for 'larger the better' condition.

Trials	A	B	C	Area (mm^2)	Leg length (mm)	Load resistance (Ω)	Efficiency (in %)	S/N (for efficiency)	Power (W)	S/N (for power)
1	1	1	1	2	2	6	13.0	22.27	31.33	29.92
2	1	2	2	2	3	7	12.8	22.14	22.16	26.91
3	1	3	3	2	4	8	12.4	21.86	16.91	24.56
4	1	4	4	2	5	9	12.0	21.56	13.65	22.70
5	1	5	5	2	6	10	11.6	21.33	11.34	21.09
6	2	1	2	2.5	2	7	13.2	22.39	26.62	28.50
7	2	2	3	2.5	3	8	13.1	22.38	26.03	28.30
8	2	3	4	2.5	4	9	13.1	22.34	20.55	26.26
9	2	4	5	2.5	5	10	12.9	22.20	16.91	24.56
10	2	5	1	2.5	6	6	10.7	20.58	13.04	22.30
11	3	1	3	3	2	8	11.9	21.54	36.74	31.30
12	3	2	4	3	3	9	12.8	22.15	28.62	29.14
13	3	3	5	3	4	10	13.1	22.33	23.24	27.32
14	3	4	1	3	5	6	12.3	21.83	20.03	26.03
15	3	5	2	3	6	7	12.1	21.69	16.87	24.54
16	4	1	4	3.5	2	9	10.9	20.73	37.10	31.39
17	4	2	5	3.5	3	10	12.1	21.64	29.91	29.51
18	4	3	1	3.5	4	6	13.3	22.48	28.89	29.21
19	4	4	2	3.5	5	7	13.1	22.37	23.59	27.45
20	4	5	3	3.5	6	8	12.9	22.24	19.94	25.99
21	5	1	5	4	2	10	9.8	19.83	36.36	31.21
22	5	2	1	4	3	6	13.2	22.44	39.60	31.95
23	5	3	2	4	4	7	13.4	22.53	31.45	29.95
24	5	4	3	4	5	8	13.3	22.51	26.02	28.31
25	5	5	4	4	6	9	13.2	22.44	22.19	26.92
Average							12.5	21.91	24.76	27.42

respectively. The optimized results using Eq. (17) have been found to be 41.8 W power and 13.6% efficiency. The difference in the simulated and predicted results for efficiency and power output have been estimated as 5.8% and 14%, respectively. The 95% CI calculated as per Eq. (18) for efficiency and power are ± 3% and ± 6.3 W. Thus, the simulated results under optimized conditions should lie in the range from 10.6% to 16.6% efficiency and from 35.5 W to 48.1 W power output. Performing FEM for the TEG with optimized combinations of design parameters, we have predicted with 95% CI the maximum efficiency of 12.83% and the maximum power output as 48 W. It suggests ~52% increase in power output after performing the optimization process by Taguchi method.

It is to be noted that the maximum efficiency and maximum power output in TEG have never been obtained for the same combination of various control factors. To obtain the desired combination of efficiency

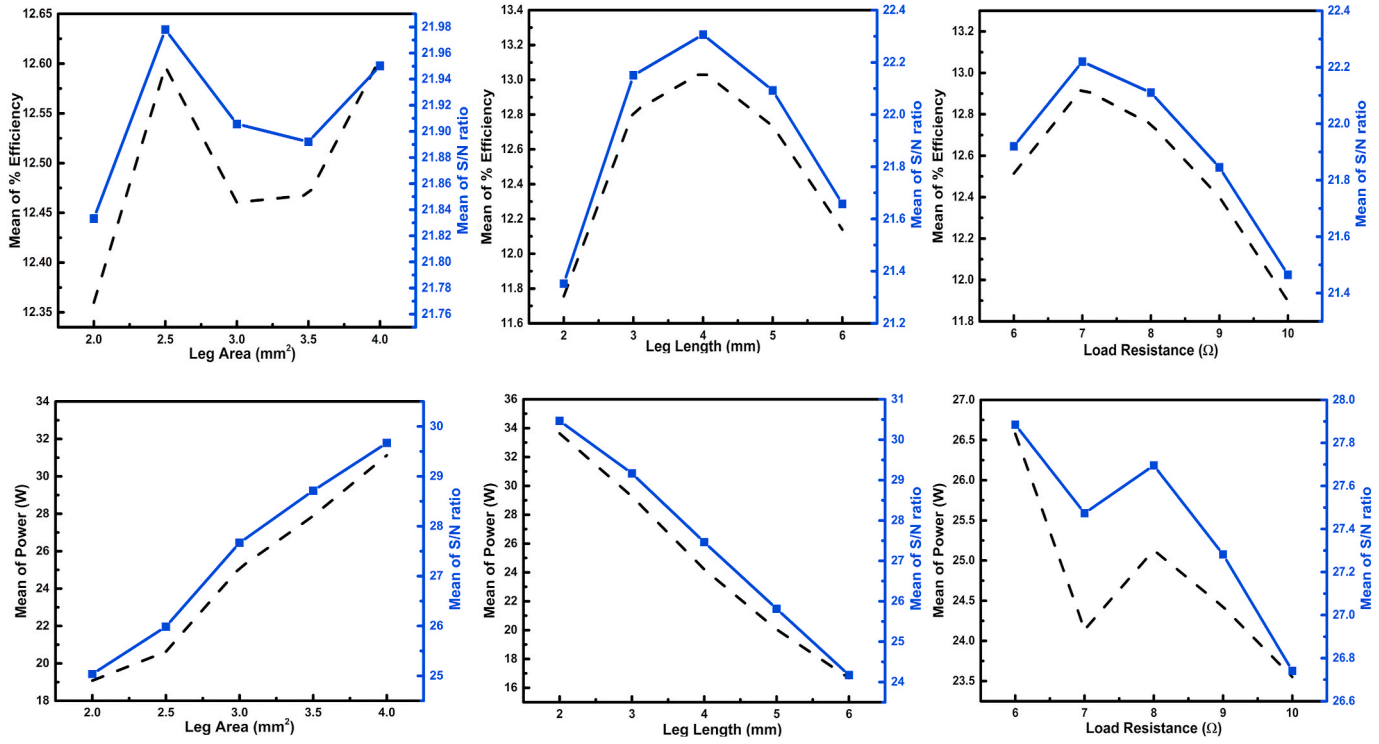

Fig. 4. Taguchi analysis, mean value of raw data (shown in black dashed line) and means of their S/N ratio (shown in solid blue line) for different control factors such as leg area, leg length, and load resistance. The upper half is plotted for efficiency and the bottom half is for power. (For interpretation of the references to colour in this figure legend, the reader is referred to the Web version of this article.)

and power output in TEG with optimized configuration, a weighting factor, w has been further introduced [20] for calculating the combined S/N ratio as depicted by Eq. (19).

$$\text{Larger the better } (S/N) = -10\log\left[\frac{1}{R}\sum_{i=1}^{R}\left[\frac{w}{y_i^2}+\frac{1-w}{z_i^2}\right]\right] \quad (19)$$

Where, y_i and z_i are raw datas for power and efficiency, respectively. The values for different weighting factor along with the optimal settings are shown in Table 4. The mean S/N response against different levels of control factors is plotted in Fig. 5 and presented in Table S3 in the Supporting Information.

ANOVA analysis table for efficiency is shown in Table 5. The contribution of the control factors as presented in Table 5 is in the order of leg length (27.37%), load resistance (14.86%) and leg area (1.03%); but the error gives the maximum contribution (56.73%). Such high contribution from error suggests that efficiency depends on other factors as well such as the plate area, leg spacing etc. which have not been considered in this study. Therefore, error term contributes mostly to the efficiency, followed by leg length, load resistance and leg area respectively. ANOVA analysis shown in Table 6 for power output suggests the percentage contribution of leg length (61.86%) to be maximum followed by leg area (31.02%) and the load resistance (1.78%). Error term contributes to only 3.33% which is again due to the other unaccounted factors. Chen et al. [13] has used factor effect value to analyze the effect of factors on the output power and efficiency. Effect for each factor can be calculated as the difference between maximum and minimum value of mean S/N ratios. A higher effect value suggests higher impact of that factor. Factor effect values for efficiency and power output values has been reported in Fig. S3. The order of factors influencing efficiency can be written as B (Leg length) > C (Load Resistance) > A (Leg Area) and that for power as B > A > C. This order in result matches with what has been obtained from ANOVA analysis thus suggesting the order to be true. Thus, leg length has the highest impact on efficiency and power output of TEG under isothermal heat source condition.

3.3. Performance optimization under isoflux heat source condition

3.3.1. Leg geometry optimization

We have further investigated performance of TEG under isoflux heat source condition. A heat flux of 63 kW/m^2 has been chosen so that the maximum obtained temperature at the hot side doesn't exceed 800 K as the material property above 800 K is not known. The TEG leg geometry has been optimized for maximum power output and efficiency similarly as considered in the isothermal condition. Since, the efficiency as defined in Eq. (2) equals to the ratio of power output to heat going into the TEG, the efficiency and power output values will follow the identical trend for varying combination of TEG design parameters in isoflux heat source condition. The results obtained are plotted in Fig. 6a. It is evident that the TEG with the leg geometry of pyramid-up demonstrates a maximum energy conversion followed by cone-up, cone-down, pyramid-down, cylindrical and square base leg geometry. Maximum power output has been estimated as 5.1 W after geometry optimization of TEG for pyramid-up configuration. Temperature distribution within the pyramid-up legged TEG at 5 Ω is shown in Fig. 6b. Constant heat flux falling on the top substrate is not distributed uniformly within the TE legs, instead the maximum heat inflow is at the edges thus enhancing the temperature of the edges as is evident from Fig. 6b.

We have further optimized other control parameters such as cross-sectional area of the leg, leg length and load resistance using Taguchi and ANOVA methods. Since, the area ratio of top and bottom ends in conical and pyramid frustum legs are kept either 2 or ½, only top end area has been chosen as the controlling factors instead of choosing both the top and bottom end areas separately. Further, increasing the trapezoidity or leg area ratio to 4, we have been able to enhance the efficiency, as shown in figure labelled pyramid-up A4 in Fig. 6a. However, this leg geometry (pyramid-up A4) has not been chosen for further optimization based on the assumption of maintaining the structural integrity of the TEG and we have used pyramid-up leg geometry.

Table 4
Optimal setting condition for combined effect of maximum efficiency and maximum power at different weight factors.

Weight factor (w)	Optimal setting condition
w = 0	$A_5B_1C_1$
w = 0.1	$A_5B_1C_3$
w = 0.2	$A_5B_2C_2$
w = 0.8	$A_5B_3C_2$
w = 0.9	$A_5B_3C_2$
w = 1	$A_2B_3C_2$

3.3.2. Optimization of control factors using Taguchi and ANOVA analysis

For Taguchi and ANOVA analysis, the control factors have been chosen at 5 different levels in the given range for leg area of top end (2–4 mm^2), leg length (1–3 mm) and load resistance (4–8 Ω) as presented in Table 7.

The L_{25} orthogonal array along with the values of efficiency, power, their S/N ratios and maximum hot side temperature detected are shown in Table 8. The corresponding mean response for efficiency and mean response of its S/N ratios are shown in Table S4 respectively. The plots of means and S/N ratio at all levels of different control factors are shown in Fig. 7. It is to be noted that while optimizing geometrical parameters the maximum temperature has reached as high as 1050 K shown in trial no. 5 (marked bold). It can be fatal for TEG as the chalcogenides which are used as TE material melts or evaporates at such high temperature. Hence such combination of parameters must be avoided in designing when the incoming heat flux is as high as 63 kW/m^2. Further, similar study carried out at a lower heat flux, 50 kW/m^2 has rendered the same results but with reduced hot side maximum temperature as described in Supporting Information.

The trends in S/N ratio for power suggests that under isoflux heat source conditions, power increases with decreasing leg area and increasing leg length which is opposite of what has been observed for isothermal condition. The S/N plots in Fig. 7 reveals the optimum condition setting for maximum performance to be $A_1B_5C_2$ i.e. a top leg area of 2 mm^2, leg length of 3 mm and load resistance of 5 Ω. The optimized results using Eq. (17) has been calculated to be 13.1%. The confidence interval (CI) of 95% for the predicted efficiency has been estimated using Eq. (18), which denotes that optimized efficiency should lie between 10.3% and 15.8%. Using optimum conditions ($A_1B_5C_2$) we have further carried out the finite element simulation to estimate the optimized efficiency under isoflux heat source and it has been found to be 10.6%, which falls in the range predicted with the 95% CI validating our optimization method. At the optimized condition, 10.6 W power has been obtained in the simulations, which is ~100% enhancement due to optimization process.

As defined by Lohninger [36], S/N ratio refers to the ratio of the mean of raw data to the noise created in the raw data. This noise can be due to a number of uncontrolled (or here unaccounted) parameters. The trend in the S/N plot for load resistance is maximum at 5 Ω with minimum noise but the mean of raw data is showing maxima at 8 Ω with the lowest S/N ratio suggesting a higher noise (or highest effect of uncontrolled factors). Hence one needs to choose cautiously. The optimum value of load resistance would be 5 Ω while 8 Ω load resistance yields maximum efficiency of 15.15% within the chosen values of leg dimensions and load resistance. ANOVA analysis table is shown for efficiency in Table 9. It is evident from ANOVA analysis; leg length contributes the maximum (78%) followed by leg area (17.43%) and load resistance (1.39%). The error term has contribution of 3.11%. Factor effect value has been plotted in Fig. S4 which suggests that the impact of control factors is in the order B (leg length) > A (leg area) > C (load resistance). This order matches with what has been obtained from

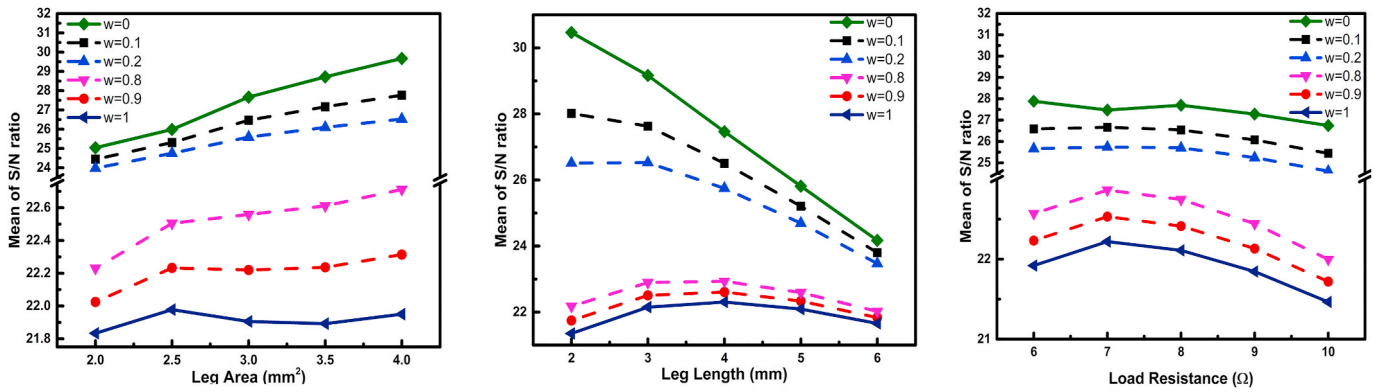

Fig. 5. S/N response plotted for optimal setting of both efficiency and power output at different weight factor (w) against different levels of control factors such as leg area, leg length, and load resistance.

Table 5
ANOVA analysis table for efficiency.

Source	Degrees of Freedom	Sum of Squares	Variance	F-value	Percentage contribution
A) Leg Area	4	0.21	0.053	0.05	1.03
B) Leg length	4	5.69	1.42	1.45	27.37
C) Load resistance	4	3.09	0.77	0.79	14.86
Error	12	11.79	0.98		56.73
Total	24	20.77			100

Table 6
ANOVA analysis table for power output.

Source	Degrees of Freedom	Sum of Squares	Variance	F-value	Percentage contribution
D) Leg Area	4	498.89	124.72	29.76	33.02
E) Leg length	4	934.72	233.68	55.76	61.86
F) Load resistance	4	27	6.75	1.61	1.78
Error	12	50.29	4.19		3.33
Total	24	1510.89			100

ANOVA analysis. Therefore, leg length has the highest impact under isoflux (constant heat) and isothermal heat source condition.

The results in the current study have been obtained upon assuming constant or fixed values of some parameters such as contact resistance, emissivity etc. The results obtained after optimization are liable to change in the real scenario as the values of these parameters may change. The contact resistance values may be affected by applied contact pressure, roughness of the surfaces, interfacial layer material properties, fabrication routes and operating conditions. Emissivity values are also subject to surface roughness, temperature, dirt and foreign body on the surface.

Based on operational process, the exhaust gases, flue gases, hot gases released from chimney, etc. may have constant temperature over a period of time scale. Basically, it is a constant heat flux but is sometimes called constant temperature source (Isothermal) and we get an inferior power generation from the optimized TEG. Therefore, we should always consider the heat source as isoflux condition. Pyramid up legged TEG has been obtained as optimized leg geometry in case of isoflux condition and it also shows highest efficiency for isothermal case. Thus, pyramid up geometry should be chosen as the optimal geometry in the real condition. As discussed earlier, the temperature distribution in isoflux case is not uniform and decreases as we move from edge to the center of the TEG. For example, as shown in Fig. S6, the temperature is uniform at

Table 7
Control factors and their levels assumed under isoflux heat source condition.

Control Factors		units	Level 1	Level 2	Level 3	Level 4	Level 5
A	Leg cross sectional area of top end	mm^2	2	2.5	3	3.5	4
B	Leg length	mm	1	1.5	2	2.5	3
C	Load resistance	Ω	4	5	6	7	8

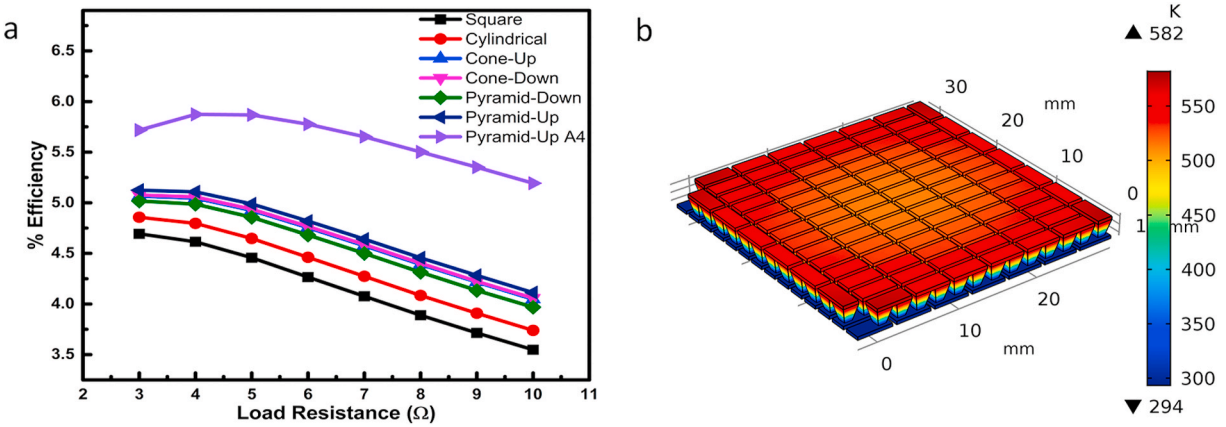

Fig. 6. (a) Performance evaluation of modelled TEG for varying leg geometries under isoflux condition (b) Temperature distribution in pyramid-up legged TEG modelled for geometry optimization under isoflux condition at 5 Ω.

Table 8
The results (efficiency and power output) of the simulation as per the orthogonal array, their S/N ratio for 'larger is better' condition along with maximum temperature obtained within the TEG is shown.

Trials	A	B	C	Area (mm^2)	Leg length (mm)	Load resistance (Ω)	Efficiency (in %)	S/N (for efficiency)	Power (W)	S/N (for power)	T_h [Max Temp. at Hot End](K)
1	1	1	1	2	1	4	3.8	11.64	3.85	11.71	567
2	1	2	2	2	1.5	5	6.6	16.43	6.68	16.50	656
3	1	3	3	2	2	6	8.9	18.97	8.96	19.04	741
4	1	4	4	2	2.5	7	10.5	20.43	10.59	20.50	835
5	1	5	5	2	3	8	15.1	23.61	15.27	23.68	**1050**
6	2	1	2	2.5	1	5	2.7	8.55	2.69	8.62	523
7	2	2	3	2.5	1.5	6	5.3	14.47	5.33	14.54	602
8	2	3	4	2.5	2	7	8.0	18.07	8.07	18.14	680
9	2	4	5	2.5	2.5	8	10.4	20.38	10.53	20.45	756
10	2	5	1	2.5	3	4	8.9	19.04	9.03	19.11	826
11	3	1	3	3	1	6	1.8	5.11	1.81	5.18	486
12	3	2	4	3	1.5	7	3.9	11.83	3.94	11.90	558
13	3	3	5	3	2	8	6.5	16.27	6.56	16.34	629
14	3	4	1	3	2.5	4	8.2	18.22	8.22	18.29	664
15	3	5	2	3	3	5	10.2	20.17	10.28	20.24	746
16	4	1	4	3.5	1	7	1.2	1.85	1.25	1.92	458
17	4	2	5	3.5	1.5	8	2.8	8.97	2.83	9.04	522
18	4	3	1	3.5	2	4	5.6	14.98	5.66	15.05	565
19	4	4	2	3.5	2.5	5	7.7	17.72	7.75	17.79	624
20	4	5	3	3.5	3	6	10.1	20.09	10.19	20.16	694
21	5	1	5	4	1	8	0.9	−1.25	0.87	−1.18	434
22	5	2	1	4	1.5	4	2.9	9.15	2.89	9.21	481
23	5	3	2	4	2	5	4.6	13.27	4.65	13.34	536
24	5	4	3	4	2.5	6	6.6	16.45	6.70	16.52	591
25	5	5	4	4	3	7	9.2	19.27	9.26	19.34	654
Average							6.5	14.55	6.55	14.62	

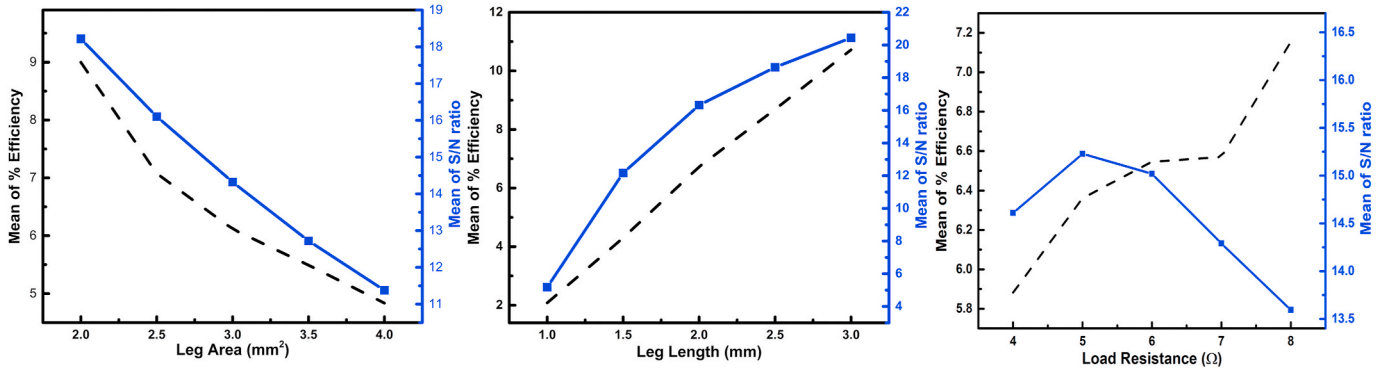

Fig. 7. Taguchi analysis, mean value of raw data and S/N ratio plotted for different control factors.

Table 9
ANOVA analysis table for efficiency under isoflux heat flow condition.

Source	Degrees of Freedom	Sum of Squares	Variance	F-value	Percentage contribution
G) Leg Area	4	52.53	13.13	16.81	17.43
H) Leg length	4	235.16	58.79	75.24	78.06
I) Load resistance	4	4.19	1.05	1.34	1.39
Error	12	9.38	0.78		3.11
Total	24	301.25			100

796 K at top of the TEG in case of optimized cylindrical legged geometry for isothermal heat source condition, the power generation in this has be obtained to be 48 W. While for the similar geometry when simulated at isoflux condition (63 kW/m^2) shows the top end temperature variation in range 418-409 K and thus the power generation is found to be ~2 W. Now considering the optimized pyramid up legged geometry for isoflux condition when simulated at 63 kW/m2, shows temperature variation in range 1000-911 K with power generation of 10.6 W. This TEG configuration when simulated at 50 kW/m^2 showed a top end temperature variation in range 812-718 K with power generation of 6.7 W. The average heat flux obtained in isothermal case is of the order of 10^5 W/m^2 and if we try to simulate assuming this heat flux, the maximum temperature of the TEG may go beyond the material defined temperature at which TE legs will melt. This further implies that the heat fluxes will be so high that it may damage the TEG.

4. Conclusions

In summary, a 3D model of TEG constituting 196 legs has been extensively studied by finite element method (FEM) for various energy losses. Power generation when considering only contact losses has been found to be lowest compared to other parasitic heat losses such as conduction, radiation or their combined effects. The TEG under all energy losses, is further optimized for leg geometry and other controlling parameters such as leg length, leg area and load resistance in order to obtain maximum performance under both isothermal as well as isoflux heat source conditions. For isothermal condition, keeping hot end temperature fixed at 800 K, the maximum power output has been obtained for cylindrical legs in our FEM study. We have further optimized

various parameters of TEG using Taguchi and ANOVA methods, which reveals a power output of 48 W and a maximum efficiency of 12.8%. The combinations of 4 mm^2 leg area, 2 mm leg length and 6 Ω load resistance have been predicted as the optimum combinations for maximizing power output.

For isoflux heat source condition, a constant heat flux of 63 kW/m^2 has been considered and geometry optimization reveals that pyramid-up design of TE legs exhibit the highest TE performance. The pyramid-up geometry on further analysis shows that the efficiency increases with increasing leg area ratio. Our optimization study implies that 10.6 W power with a conversion efficiency of 10.6% can be achieved under this isoflux heat source condition for the pyramid-up geometry with the combinations of 2 mm^2 leg area, 3 mm leg length and 5 Ω load resistance. Our simulation results after performing optimization process have shown 52% and 100% increase in maximum power output for isothermal and isoflux conditions, respectively, which will enable researchers to design and fabricate high performance TEG for clean energy generation from waste heat.

CRediT authorship contribution statement

Mani Ranjan: Supervision, performed the simulation under supervision of T.M. M.R. **Tanmoy Maiti:** Formal analysis, Writing - original draft, was responsible for the original research concept and design of experiment. analysed the data and wrote the manuscript.

Declaration of competing interest

The authors declare that they have no known competing financial interests or personal relationships that could have appeared to influence the work reported in this paper.

Acknowledgements

The authors acknowledge the financial supports from the Indian Space Research Organization (ISRO) under Grant STC/MET/2018112.

Appendix A. Supplementary data

Supplementary data to this article can be found online at https://doi.org/10.1016/j.jpowsour.2020.228867.

References

[1] C.B. Field, Climate Change 2014–Impacts, Adaptation and Vulnerability: Regional Aspects, Cambridge University Press, 2014.
[2] A. Firth, B. Zhang, A. Yang, Quantification of global waste heat and its environmental effects, Appl. Energy 235 (2019) 1314–1334.
[3] S. Kumar, S.D. Heister, X. Xu, J.R. Salvador, G.P. Meisner, Thermoelectric generators for automotive waste heat recovery systems part ii: parametric evaluation and topological studies, J. Electron. Mater. 42 (2013) 944–955.
[4] C. Hadjistassou, E. Kyriakides, J. Georgiou, Designing high efficiency segmented thermoelectric generators, Energy Convers. Manag. 66 (2013) 165–172.
[5] Z. Tang, Y. Deng, C. Su, W. Shuai, C. Xie, A research on thermoelectric generator's electrical performance under temperature mismatch conditions for automotive waste heat recovery system, Case Studies in Thermal Engineering 5 (2015) 143–150.
[6] H.S. Kim, W. Liu, G. Chen, C.-W. Chu, Z. Ren, Relationship between thermoelectric figure of merit and energy conversion efficiency, Proc. Natl. Acad. Sci. Unit. States Am. 112 (2015) 8205–8210.
[7] X. Hu, A. Yamamoto, M. Ohta, H. Nishiate, Measurement and simulation of thermoelectric efficiency for single leg, Rev. Sci. Instrum. 86 (2015), 045103.
[8] R. Bjørk, D.V. Christensen, D. Eriksen, N. Pryds, Analysis of the internal heat losses in a thermoelectric generator, Int. J. Therm. Sci. 85 (2014) 12–20.
[9] D. Ebling, K. Bartholomé, M. Bartel, M. Jägle, Module geometry and contact resistance of thermoelectric generators analyzed by multiphysics simulation, J. Electron. Mater. 39 (2010) 1376–1380.
[10] P. Ziolkowski, P. Poinas, J. Leszczynski, G. Karpinski, E. Müller, Estimation of thermoelectric generator performance by finite element modeling, J. Electron. Mater. 39 (2010) 1934–1943.
[11] U. Erturun, K. Erermis, K. Mossi, Effect of various leg geometries on thermo-mechanical and power generation performance of thermoelectric devices, Appl. Therm. Eng. 73 (2014) 128–141.
[12] A.Z. Sahin, B.S. Yilbas, The thermoelement as thermoelectric power generator: effect of leg geometry on the efficiency and power generation, Energy Convers. Manag. 65 (2013) 26–32.
[13] W.-H. Chen, S.-R. Huang, Y.-L. Lin, Performance analysis and optimum operation of a thermoelectric generator by Taguchi method, Appl. Energy 158 (2015) 44–54.
[14] R. Anant Kishore, P. Kumar, M. Sanghadasa, S. Priya, Taguchi optimization of bismuth-telluride based thermoelectric cooler, J. Appl. Phys. 122 (2017), 025109.
[15] R.A. Kishore, P. Kumar, S. Priya, A comprehensive optimization study on Bi 2 Te 3-based thermoelectric generators using the Taguchi method, Sustainable Energy & Fuels 2 (2018) 175–190.
[16] R. Deng, X. Su, S. Hao, Z. Zheng, M. Zhang, H. Xie, et al., High thermoelectric performance in Bi 0.46 Sb 1.54 Te 3 nanostructured with ZnTe, Energy Environ. Sci. 11 (2018) 1520–1535.
[17] H. Lee, J. Sharp, D. Stokes, M. Pearson, S. Priya, Modeling and analysis of the effect of thermal losses on thermoelectric generator performance using effective properties, Appl. Energy 211 (2018) 987–996.
[18] Z. Ouyang, D. Li, Modelling of segmented high-performance thermoelectric generators with effects of thermal radiation, electrical and thermal contact resistances, Sci. Rep. 6 (2016) 24123.
[19] E. Thacher, Heat loss and thermoelectric generator design, Energy Convers. Manag. 25 (1985) 519–525.
[20] R.A. Kishore, M. Sanghadasa, S. Priya, Optimization of segmented thermoelectric generator using Taguchi and ANOVA techniques, Sci. Rep. 7 (2017) 16746.
[21] J.-Y. Jang, Y.-C. Tsai, Optimization of thermoelectric generator module spacing and spreader thickness used in a waste heat recovery system, Appl. Therm. Eng. 51 (2013) 677–689.
[22] S. Athreya, Y. Venkatesh, Application of Taguchi method for optimization of process parameters in improving the surface roughness of lathe facing operation, International Refereed Journal of Engineering and Science 1 (2012) 13–19.
[23] A.C. Alkidas, P.A. Battiston, D.J. Kapparos, Thermal studies in the exhaust system of a diesel-powered light-duty vehicle, SAE Trans. 113 (2004) 164–181.
[24] R. Pundir, G. Chary, M. Dastidar, Application of Taguchi method for optimizing the process parameters for the removal of copper and nickel by growing Aspergillus sp, Water resources and industry 20 (2018) 83–92.
[25] G. Tan, F. Shi, S. Hao, L.-D. Zhao, H. Chi, X. Zhang, et al., Non-equilibrium processing leads to record high thermoelectric figure of merit in PbTe–SrTe, Nat. Commun. 7 (2016) 12167.
[26] K.F. Hsu, S. Loo, F. Guo, W. Chen, J.S. Dyck, C. Uher, et al., Cubic AgPbmSbTe2+m: bulk thermoelectric materials with high figure of merit, Science 303 (2004) 818–821.
[27] G.J. Snyder, E.S. Toberer, Complex thermoelectric materials, in: Materials for Sustainable Energy: A Collection of Peer-Reviewed Research and Review Articles from Nature Publishing Group, World Scientific, 2011, pp. 101–110.
[28] Y. Yang, S. Xie, F. Ma, J. Li, On the effective thermoelectric properties of layered heterogeneous medium, J. Appl. Phys. 111 (2012), 013510.
[29] M. Jaegle, Multiphysics simulation of thermoelectric systems-modeling of Peltier-cooling and thermoelectric generation, COMSOL Conference (6) (2008). Conference Proceedings Record Number: 22.
[30] Y. Mizuguchi, A. Omachi, Y. Goto, Y. Kamihara, M. Matoba, T. Hiroi, et al., Enhancement of thermoelectric properties by Se substitution in layered bismuth-chalcogenide LaOBiS2-x Se x, J. Appl. Phys. 116 (2014) 163915.
[31] G. Taguchi, S. Konishi, S. Konishi, Taguchi Methods: Orthogonal Arrays and Linear Graphs. Tools for Quality Engineering, American Supplier Institute Dearborn, MI, 1987.
[32] R.K. Roy, Design of Experiments Using the Taguchi Approach: 16 Steps to Product and Process Improvement, John Wiley & Sons, 2001.
[33] Wp Yang, Y. Tarng, Design optimization of cutting parameters for turning operations based on the Taguchi method, J. Mater. Process. Technol. 84 (1998) 122–129.
[34] P.J. Ross, P.J. Ross, Taguchi Techniques for Quality Engineering: Loss Function, Orthogonal Experiments, Parameter and Tolerance Design, McGraw-Hill, New York, 1988.
[35] R.A. Fisher, Statistical Methods for Research Workers. Breakthroughs in Statistics, Springer, 1992, pp. 66–70.
[36] H. Lohninger, Fundamentals of Statistics, vol. 5, Retrieved December, 2010, 2010.